Systems & Control Transactions

Research Article - Peer Reviewed Conference Proceeding
ESCAPE 35 - European Symposium on Computer Aided Process Engineering
Ghent, Belgium. 6-9 July 2025
Jan F.M. Van Impe, Grégoire Léonard, Satyajeet S. Bhonsale,
Monika E. Polańska, Filip Logist (Eds.)

PSE PRESS

Model-based approach to template-induced macromolecule crystallisation

Daniele Pessina[a,b], Jorge Calderon de Anda[c], Claire Heffernan[c], Tony Tian[c], Oliver Watson[c], Jerry Y. Heng[a,d] and Maria M. Papathanasiou[a,b,*]

[a] Sargent Centre for Process Systems Engineering, Imperial College London, SW7 2AZ, United Kingdom
[b] Department of Chemical Engineering, Imperial College London, SW7 2AZ, United Kingdom
[c] Chemical Development, Pharmaceutical Technology & Development, Operations, AstraZeneca, Macclesfield 9 SK10 2NA, U.K.
[d] Institute of Molecular Science, Department of Chemical Engineering, Imperial College London, SW7 2AZ, United Kingdom
* Corresponding Author: maria.papathanasiou11@imperial.ac.uk

ABSTRACT

Biomacromolecules have intricate crystallisation behaviour due to their size and many interactions in solution and can often only crystallise in narrow ranges of experimental conditions. High solute concentrations are needed for crystal nucleation and growth, exceeding those eluted upstream and therefore preventing the adoption of crystallisation in downstream separation steps. By promoting molecular aggregation and nucleation via a lowered energy barrier, heterogeneous surfaces or templates can relax the supersaturation requirements and widen the crystallisation operating space. Though templates are promising candidates for process optimisation, their experimental testing has generally been limited to small-volume experiments, and quantification of their impact on process intensification and quality metrics at higher volumes remains unexplored. To address the knowledge gap, a model-based investigation of template-induced protein crystallisation systems through evaluation of key metrics is presented. Porous silica nano-particles with three chemical functionalisations (hydroxyl, carboxyl and butyl) are added to batch lysozyme crystallisation experiments at 40ml. Crystallisation population balance models are parametrised with an experimentally-validated parameter estimation methodology and further experiments are simulated. The templates appear to lower the estimated interfacial energy compared to the homogeneous case, leading to nucleation rate profiles which are less dependent on supersaturation. For this reason, the templates can crystallize quicker than the homogeneous system, particularly at lower initial concentrations. The simulation results highlight the ability of heteronucleants to alter nucleation rate profiles, and their potential to be used as process optimisation and intensification tools for biomacromolecule purification.

Keywords: Protein crystallisation, Template-induced nucleation, Population-balance modelling

INTRODUCTION

Advanced therapeutic proteins, such as monoclonal antibodies and immunoglobins are effective at treating many chronic medical conditions [1]. Their increased demand and improvements in their upstream manufacturing have indicated the need for intensified and cost-effective downstream protein purification [2, 3]. Chromatographic units, currently able to separate the therapeutic proteins at very high purity, remain expensive, difficult to scale-up and have a significant environmental footprint [4]. It is therefore critical to identify alternative and more efficient purification methods that reduce costs and improve consumer access to the novel therapies being released on the market.

The majority of small-molecule active pharmaceutical ingredients (APIs) are purified through crystallisation, a first-order phase transition in which a highly pure, thermodynamically stable and easily filterable solid is formed in solution [5]. Crystalline formulations offer improved stability, purity, handling and storage compared to chromatography separation alternatives [6]. Due to the protein's size, structural flexibility and many sources of chemical interaction, the macromolecules often only

crystallise in narrow ranges of conditions, which are firstly difficult to identify and secondly restrict the crystalliser's operational flexibility [7]. High energetic barriers are associated with crystal nucleation since the proteins must rotate and fold to rearrange themselves into the ordered crystal lattice, requiring strong thermodynamic driving forces and high supersaturations. It is important to highlight that the minimum solute concentrations needed for crystallisation exceed those eluted by upstream processes prior to any purification steps [8]. Therefore, processes designed to produce solid formulations of advanced therapeutics require concentrating chromatographic purification steps before crystallisation becomes thermodynamically possible. If, however, minimum concentration requirements for crystallisation can be relaxed and low-supersaturation nucleation is facilitated, chromatographic units can be avoided to improve scale-up, costs and the environmental footprint of the processes.

Template-induced nucleation involves the use of additives in the crystallisation solution to favour molecular rearrangement into a nucleus through three methods: functional group matching, epitaxy, and topographic features [9]. Soft templates are dissolved additives, such as amino acids [10], which disrupt the protein's hydration layer and enhance favourable protein-protein interactions. Hard templates instead are un-dissolved, heterogeneous surfaces which, particularly through complementary surface chemistries and porous structures, promote protein aggregation and concentrate the protein to induce higher local supersaturations. Many template types have been shown to act as nucleation enhancers to lower concentration requirements for nucleation, as well as preferentially crystallising specific polymorphs [10–15]. However, template-induced nucleation investigations have generally been limited to small-volume studies to obtain diffraction-quality protein crystals [2], and there is a lack of reliable, quantitative information describing both how templates affect crystallisation kinetics and the extent to which template addition can drive process intensification. To the authors' knowledge, no comprehensive studies on the effect of templates on kinetic parameters and the crystallisation operating space have been published, and their impact on crystallisation process design remains uncertain. Fully-experimental characterisation of crystallisation kinetics requires time consuming and costly experiments, and solution volumes must be reduced to prevent excessive API use [16]. Population-balance models (PBMs) can be used to support the experimental campaign and accelerate process development with fewer, larger-scale experiments [17, 18]. Once the PBMs are parametrised, aspects of the crystallisation process such as nucleation rate, yield and crystal size profiles, which might be experimentally unavailable or costly to measure at scale, can be quickly queried through model simulations. By probing the PBMs for multiple crystalliser conditions, operating spaces of template-induced nucleation systems can be identified and assessed to support template adoption for pharmaceutical manufacturing. While previous studies on template-assisted protein crystallisation have studied templated-nucleation probabilities [8, 19], to the author's knowledge this is the first investigation of template-assisted nucleation that integrates PBMs to assess how the surfaces affect the operating spaces and support scale-up by aiding the selection of optimal initial conditions and residence times.

To this end, a model-based evaluation of template-induced protein crystallisation operating spaces is presented in this work. Lysozyme is crystallised homogeneously and in the presence of functionalised porous silica nano-particles (SNPs) at 40ml. PBMs are parametrised and used for high-throughput *in-silico* experimentation. The regressed models indicate that particularly at lower initial concentrations, template-induced nucleation is quicker and less dependent on supersaturation compared to the homogeneous system.

METHODOLOGY

Experimental protocol for lysozyme crystallisation

Lysozyme anti-solvent crystallisation experiments are performed at 40ml in a stirred batch crystalliser ($T = 20℃$, 0.1M sodium acetate buffer, pH $= 4.2$, [NaCl] $=$ 50 mg/ml, 75 rpm stirring). Lysozyme is first dissolved and filtered through a 0.22μm filter to obtain buffered solutions of different lysozyme concentrations. NaCl is dissolved at 100 mg/ml concentration in the sodium acetate buffer to prepare the anti-solvent solution. Crystallisation starts by mixing equal volumes of the protein and precipitant solution. Lysozyme concentration is monitored at regular time intervals using a Thermo Fisher NanoDrop One UV-Vis spectrophotometer unit by drawing approximately 0.1ml from the broth and filtering with a 0.22μm filter to prevent the solids from affecting UV absorbance. At batch termination, the solution is filtered and dried. The collected crystals are suspended in isopropyl alcohol for laser-diffraction particle size measurements with an Anton Paar PSA 1190 unit.

Computational methodology

One-dimensional crystallisation PBMs are formulated and parametrised against the measured concentration profiles and crystal sizes to predict the crystallisation operating space. Firstly, aggregation and breakage are neglected in the population balance, a common and valid assumption for lysozyme crystallisation modelling [17, 20] (Eq. 1). Due to the balance's hyperbolic partial differential structure, the balance is solved transformed via the

Method of Moments [21], and the resulting 6 differential equations are solved in Julia, with access of model gradients though forward-mode automatic differentiation. A mass balance is included to model solute consumption (Eq. 3). Classical nucleation theory, power-law growth and negligible aggregation and breakage kinetics are assumed (Eq. 4,5). The nucleation and growth equations each require two kinetic parameters to be regressed. Parameter estimation and uncertainty quantification is carried out using a Markov Chain Monte Carlo No-U-Turn Sampler [22]. Uniform priors are used for candidate parameter sampling, and the negative log likelihood, an indicator of model mispredictions of the experimental measurements, is used to identify parameter posterior distributions. Each model was parametrised with experiments using at least two different initial conditions, and each experiment was repeated three times. Given that templates are assumed to only affect nucleation kinetics, growth parameters are estimated from template-free measurements and their posterior is fixed before template-induced nucleation parameters are estimated from their respective measurements. High-throughput *in-silico* experimentation is carried out by simulating each model for a range of initial concentrations and residence times and calculating process metrics of interest.

$$\frac{\partial n}{\partial t} + \frac{\partial (Gn)}{\partial L} = B_0 \delta (L - L_{min}) \quad (1)$$

$$S = {}^{c(t)}/_{c_{\text{sat.}}} \quad (2)$$

$$\frac{dc}{dt} = -3\rho_c k_v \int_0^\infty G n L^2 \, dL \quad (3)$$

$$\text{CNT} : B_0 = A_j S \exp\left(\frac{-16\pi\gamma^3 v_0^2}{3k_B^3 T^3 \ln^2 S}\right) \quad (4)$$

$$\text{Emp.} : G = A_g (S-1)^g \quad (5)$$

RESULTS

Each of the parameter estimation routines appear to be successful, with good agreement to the experimental measurements. The model predictions of lysozyme crystallisation with carboxyl-functionalised silica templates are shown in Figure 1. The predicted concentration trajectories accurately capture the experimentally measured trends. Both the measured and predicted trajectories appear to have low uncertainty, suggesting the models can be used to predict each system's concentration and fractional yield for a wide range of initial conditions.

The measured average particle sizes have higher uncertainty. Average particle size prediction of Measurement 1 ($C_0 = 20$ mg/ml) appears to be accurate, with overlapping uncertainty ranges (Meas. $= 5.13 \pm 1.28$ µm, Pred. $= 6.69 \pm 0.98$ µm). The model fit to Measurement 2 ($C_0 = 16$ mg/ml) instead leads to poorer prediction of the measured particle size (Meas. $= 20.17 \pm 5.04$ µm, Pred. $= 7.23 \pm 1.3$ µm). The same assessment of the model parametrisations can be made for the predictions of hydroxyl- and butyl-functionalised templated systems, whereby concentration predictions have good agreement with the measured points, and the predicted average particle size is less accurate. Although the mispredictions may be caused by inaccurate assumptions in the model formulation and parametrisation (such as restriction of growth kinetic parameters for the templated systems), the models are nonetheless valuable to assess the templates' impact on crystallisation process design, and poor understanding of template-assisted crystallisation currently prevents further investigations of more appropriate model assumptions.

Figure 1: Comparison between experimental data of

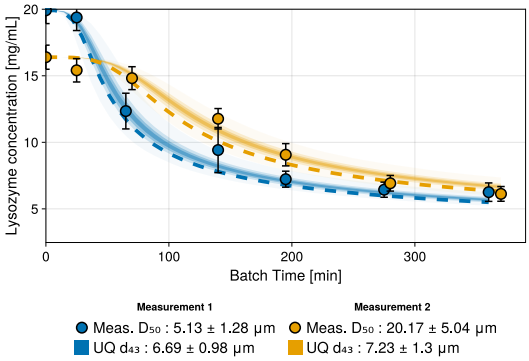

crystallisation with carboxyl-functionalised silica templates and fitted model.

The regressed nucleation parameters of each tested system are reported in Table 1. The pre-exponential nucleation constant A_j is interpreted as a function of the rate of molecular attachment to the critical nucleus, and is related to the protein's molecular mobility in solution; high A_j values indicate high attachment frequencies and the presence of many nucleation sites [23]. The surface energy γ refers to the energy of the crystal-solution interface; lower γ is associated with critical nuclei of fewer molecules [23, 24]. While CNT models have simplifying assumptions, they are nonetheless valuable tools to mechanistically interpret differences between unseeded and template-assisted nucleation through parametric comparison. Compared to the homogeneous system, lower pre-exponential constants are regressed for the templated systems, suggesting molecular attachment is less frequent or fewer nucleation sites are available.

Lower surface energy is also predicted for each templated system, suggesting that while templates slow the growth of the critical nucleus, it however has a

reduced energetic barrier, has fewer molecules and its' state transition is more thermodynamically favoured. Nucleation enhancements can be explained by the lysozyme-SNP affinity; since lysozyme has been reported to have non-specific adsorption onto hydrophobic and hydrophilic surfaces, each surface chemistry has chemical affinity to lysozyme and can induce higher local lysozyme concentrations [25]. Additionally, computational studies have shown transport into porous structures also induces higher supersaturations [26], another contributing factor towards easier lysozyme nucleation.

Table 1: Regressed nucleation and growth parameters of the unseeded and templated systems

System	A_j $[\log(\#\,m^{-3}s^{-1})s]$	γ $[mJ\,m^{-2}]$
Unseeded	39.8 ± 2.0	0.68 ± 0.022
Hydroxyl	29.9 ± 2.2	0.49 ± 0.05
Butyl	22.7 ± 0.55	0.14 ± 0.07
Carboxyl	27.4 ± 2.45	0.32 ± 0.05
Growth param.	A_g $[nm\,min^{-1}]$	g $[-]$
	0.37 ± 0.08	3.30 ± 0.14

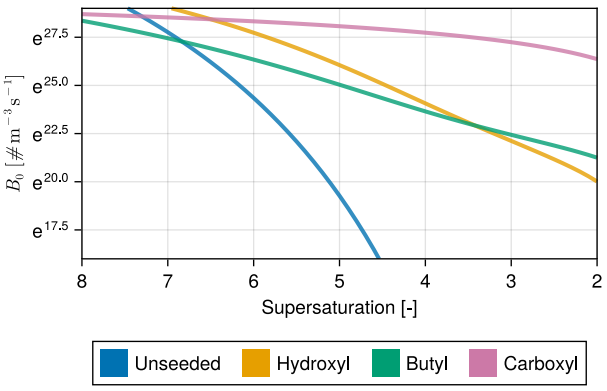

Figure 2: Calculated nucleation rate profiles for a range of supersaturations

The calculated nucleation rate profiles for a range of supersaturations (Figure 2) indicate template-induced nucleation is sustained across a wide range of supersaturations, remaining high even at $S < 4$ when homogeneous nucleation has reduced considerably. Secondly, the rates are flatter and less-dependent on supersaturation, possibly due to saturation of the templates' nucleation-enhancing effects if the templates' surface and pores are completely covered and filled with dissolved lysozyme.

After parameter estimation, simulations from each PBM are used to assess how templates alter the crystallisation operating space, with key trajectories of interest shown in Figure 3. While each system's fractional yield trajectories at intermediate and high initial concentrations ($C_0 = 17, 20$ g/L) overlap, discernible differences are calculated for systems with lower initial concentrations ($C_0 = 14$ g/L) whereby templates, and in particular the carboxylic- and butyl- functionalised SNPs, generate crystalline mass quicker than the unseeded system. Further performance metrics for this initial condition are collected in Table 2; each template reduces the time to reach 60% fractional yield, halving it in the case of butyl and carboxyl templates, and templates at-least-double the predicted crystalline mass in solution at equal residence times.

Table 2: Process metrics of each tested system with $C_0 = 14$ g/L

System	Avg. Time for 60% Frac. Yield [min]	Avg. Frac. Yield at 300 min
Unseeded	884	0.18
Hydroxyl	528 **↓-40%**	0.38 **↑+111%**
Butyl	528 **↓-40%**	0.39 **↑+116%**
Carboxyl	310**↓-65%**	0.59 **↑+228%**

The collected fractional yield and average particle size trajectories in Figure 3 show a widened crystallisation operating space towards lower initial concentrations due to the addition of templates to the crystalliser, as the templates enable low-supersaturation nucleation. The average particle size however is not solely determined by nucleation enhancements, but rather is also affected by the crystalliser's operation and the amount of solute available for crystal growth. In the case of the unseeded system, a decreasing particle size with increasing initial concentration is predicted. Since homogeneous nucleation slows considerably at lower supersaturations, systems which already start at low supersaturations have more solute mass and time for each crystal to grow, while higher initial supersaturations lead to more solute competition between nucleated crystals. An opposite trend can be observed in the case of the templated systems, caused by the sustained nucleation rate profiles, whereby the predicted average particle size slightly increases with increasing initial concentration. Since similar numbers of crystals are nucleated with each initial condition, higher initial concentrations reduce solute competition for growth by having more API mass available in solution, and lead to minor increases in the average particle size. The unseeded particle size is more sensitive to changes in initial conditions than the templated systems, highlighting templates' ability to mitigate upstream disturbances and act as crystallisation rate-limiters and controllers.

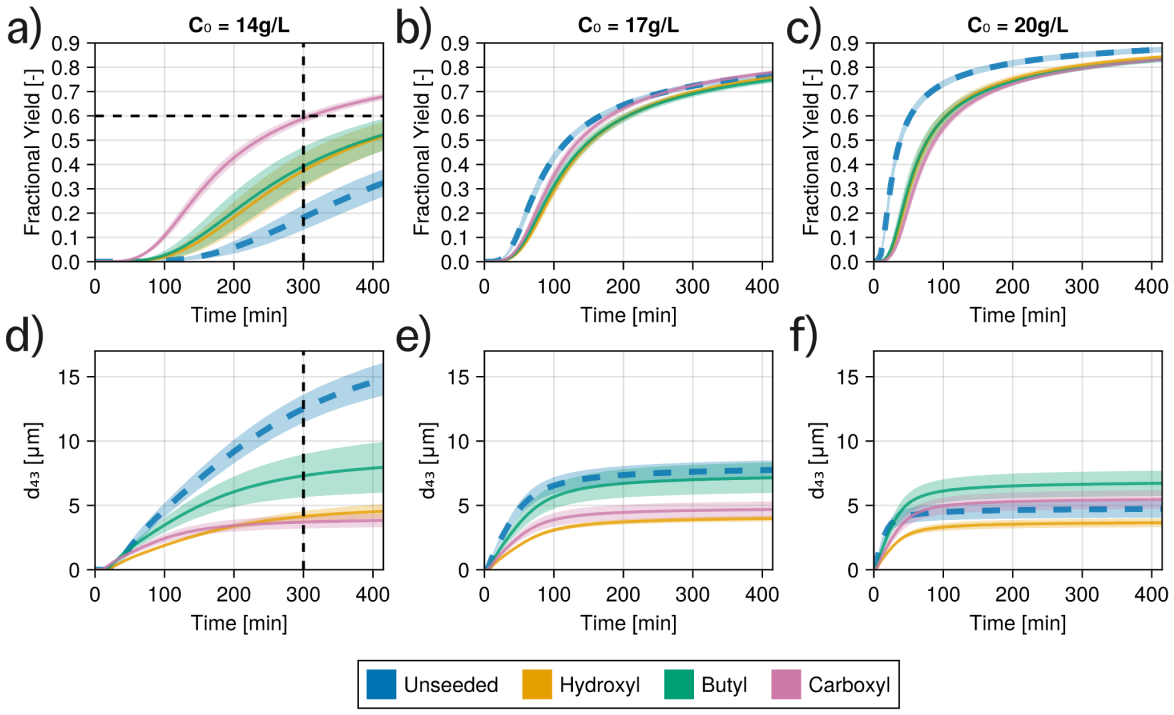

Figure 3: Fractional yield vs. residence time (a-c) and volume-weighted average particle size vs residence time (d-f) plots for three different initial concentrations

CONCLUSIONS

The adoption of crystallisation for protein purification of therapeutic manufacturing is challenged by the tight conditions in which proteins crystallise. If a solid formulation is targeted and designed for, additional purification units upstream of the crystalliser are needed which lead to increased manufacturing costs and environmental impacts.

The work presented shows that templates can be introduced to scaled-up crystallisation processes to widen the crystallisation operating space by providing a higher and more-controlled nucleation rate than the template-free system. The effect is more pronounced when the crystalliser is operated at lower initial concentrations since templates sustain nucleation at conditions where homogeneous nucleation has reduced considerably. Operating the crystalliser at lower solute concentrations is useful to facilitate control and avoid excessive nucleation or precipitation of the amorphous solute. As such, by enhancing nucleation through the addition of templates, the crystalliser's robustness can be improved to more-easily mitigate upstream disturbances, while also delivering intensified downstream purification.

REFERENCES

1. Chowdhury EA, Meno-Tetang G, Chang HY, et al (2021) Current progress and limitations of AAV mediated delivery of protein therapeutic genes and the importance of developing quantitative pharmacokinetic/pharmacodynamic (PK/PD) models. Advanced Drug Delivery Reviews 170:214–237. https://doi.org/10.1016/j.addr.2021.01.017
2. Chen W, Cheng TNH, Khaw LF, et al (2021) Protein purification with nanoparticle-enhanced crystallisation. Separation and Purification Technology 255:117384. https://doi.org/10.1016/j.seppur.2020.117384
3. Makurvet FD (2021) Biologics vs. small molecules: Drug costs and patient access. Medicine in Drug Discovery 9:100075. https://doi.org/10.1016/j.medidd.2020.100075
4. Roque ACA, Pina AS, Azevedo AM, et al (2020) Anything but Conventional Chromatography Approaches in Bioseparation. Biotechnology Journal 15:1900274. https://doi.org/10.1002/biot.201900274
5. Lemmer HJR, Liebenberg W, Lemmer HJR, Liebenberg W (2022) Crystallization: Its Mechanisms and Pharmaceutical Applications. In: Crystal Growth and Chirality - Technologies and Applications. IntechOpen
6. Rafferty J, Nagaraj H, McCloskey AP, et al (2016) Peptide Therapeutics and the Pharmaceutical Industry: Barriers Encountered Translating from the

Laboratory to Patients. Curr Med Chem 23:4231–4259. https://doi.org/10.2174/0929867323666160909155222
7. Hekmat D (2015) Large-scale crystallization of proteins for purification and formulation. Bioprocess Biosyst Eng 38:1209–1231. https://doi.org/10.1007/s00449-015-1374-y
8. McCue C, Girard H-L, Varanasi KK (2023) Enhancing Protein Crystal Nucleation Using In Situ Templating on Bioconjugate-Functionalized Nanoparticles and Machine Learning. ACS Appl Mater Interfaces 15:12622–12630. https://doi.org/10.1021/acsami.2c17208
9. Parambil JV, Poornachary SK, Heng JYY, Tan RBH (2019) Template-induced nucleation for controlling crystal polymorphism: from molecular mechanisms to applications in pharmaceutical processing. CrystEngComm 21:4122–4135. https://doi.org/10.1039/C9CE00404A
10. J. Link F, Y. Heng JY (2021) Enhancing the crystallisation of insulin using amino acids as soft-templates to control nucleation. CrystEngComm 23:3951–3960. https://doi.org/10.1039/D1CE00026H
11. de Poel W, Elemans JAAW, van Enckevort WJP, et al (2019) Epitaxial Crystallization of Insulin on an Ordered 2D Polymer Template. Chemistry – A European Journal 25:3756–3760. https://doi.org/10.1002/chem.201805276
12. Jacobo-Molina A, Clark AD, Williams RL, et al (1991) Crystals of a ternary complex of human immunodeficiency virus type 1 reverse transcriptase with a monoclonal antibody Fab fragment and double-stranded DNA diffract x-rays to 3.5-A resolution. Proc Natl Acad Sci U S A 88:10895–10899. https://doi.org/10.1073/pnas.88.23.10895
13. Kang M, Lee G, Jang K, et al (2022) Graphene Quantum Dots as Nucleants for Protein Crystallization. Crystal Growth & Design 22:269–276. https://doi.org/10.1021/acs.cgd.1c00910
14. Saridakis E, Khurshid S, Govada L, et al (2011) Protein crystallization facilitated by molecularly imprinted polymers. Proceedings of the National Academy of Sciences 108:11081–11086. https://doi.org/10.1073/pnas.1016539108
15. Verma V, Mitchell H, Errington E, et al (2023) Templated Crystallization of Glycine Homopeptides: Experimental and Computational Developments. Chemical Engineering & Technology 46:1271–1278. https://doi.org/10.1002/ceat.202200575
16. Pusey ML, Aygün RS (2017) Data Analytics for Protein Crystallization, 1st ed. 2017. Springer International Publishing : Imprint: Springer, Cham
17. Mitchell HM, Jovannus D, Rosbottom I, et al (2023) Process modelling of protein crystallisation: A case study of lysozyme. Chemical Engineering Research and Design 192:268–279. https://doi.org/10.1016/j.cherd.2023.02.016
18. Orosz Á, Szilágyi E, Spaits A, et al (2024) Dynamic Modeling and Optimal Design Space Determination of Pharmaceutical Crystallization Processes: Realizing the Synergy between Off-the-Shelf Laboratory and Industrial Scale Data. Ind Eng Chem Res 63:4068–4082. https://doi.org/10.1021/acs.iecr.3c03954
19. Gerard CJJ, Briuglia ML, Rajoub N, et al (2022) Template-Assisted Crystallization Behavior in Stirred Solutions of the Monoclonal Antibody Anti-CD20: Probability Distributions of Induction Times. Crystal Growth & Design 22:3637–3645. https://doi.org/10.1021/acs.cgd.1c01324
20. Zhou HY, Zhou GZ, Wang XZ (2022) Multi-objective optimization of protein cooling crystallization with morphological population balance models. Journal of Crystal Growth 588:126664
21. Randolph AD, Larson MA (1988) Theory of particulate processes: analysis and techniques of continuous crystallization, 2nd ed. Academic Press, San Diego
22. Hoffman MD, Gelman A (2011) The No-U-Turn Sampler: Adaptively Setting Path Lengths in Hamiltonian Monte Carlo
23. Myerson AS, Erdemir D, Lee AY (2019) Handbook of Industrial Crystallization, 3rd ed. Cambridge University Press
24. Vekilov PG (2010) Nucleation. Crystal Growth & Design 10:5007–5019. https://doi.org/10.1021/cg1011633
25. Link FJ, Errington E, Verma V, Heng JYY (2023) The role of mixing and surface hydrophobicity on the operation of a continuous tubular slug flow crystalliser for lysozyme. Chemical Engineering Journal 471:144363. https://doi.org/10.1016/j.cej.2023.144363
26. Nanev CN, Saridakis E, Chayen NE (2017) Protein crystal nucleation in pores. Sci Rep 7:35821. https://doi.org/10.1038/srep35821